MATEC Web of Conferences **88**, 03003 (2017) DOI: 10.1051/matecconf/20178803003
CBNCM 2016

Electronic and Elastic Properties of $CaMg_2$ Alloy Phase under Various Pressures by Density Functional Theory

Jia Fu[1,a,], Weihui Lin[2], Zhongren Chen[1] and Keqiang Wang[1]

[1] *Department of Material Chemistry, Southern University of Science and Technology, Shenzhen 518055, China*
[2] *School of Mechanics College, Taiyuan University of Technology, Taiyuan 030024, China*

Abstract. The influencing effect of pressure on structural, elastic and electronic properties of $CaMg_2$ Laves phase is mainly investigated. The optimized structural parameters at zero pressure are a=b=6.250Å, c=10.101Å, which has good agreement with the experimental and theoretical values. The elastic constants are calculated, and then the bulk modulus, shear modulus, Young's modulus, Poisson's ratio and anisotropy factor are determined. The results show that the applied pressure is beneficial to the elastic properties of $CaMg_2$. The analysis of electronic density of states (DOS) and Mulliken electron population reveal the bonding characteristics in $CaMg_2$ crystal. Finally, the Debye temperatures under different pressures are obtained from the average sound velocity.

1 Introduction

Magnesium alloys as low density, high specific strength, good stiffness and strength-weight ratio are widely used in aerospace industry, automobile industry, 3D printing and other fields[1,2]. Magnesium alloys can be significantly improved by adding rare-earth (RE) elements[3] and Ca element[4]. Mg-Ca alloy exhibits excellent oxidation- resistance and burning-resistance[5], and it is also regarded as one of the most promising alloy due to its appreciable corrosion resistance[6]. $CaMg_2$ Laves phase as its excellent physical and chemical properties is a typical phase in Mg-Y-Ni[7] and Mg-Al-Ca alloy[8]. Yu et al. [9] investigated the electronic structure and elastic properties of the binary AB2 type Laves phase in Mg-Al-Ca alloys. Elastic constants of $CaMg_2$ alloy are studied by Tang et al.[2]. Zhou et al. [6] has investigated the phase stability and electronic structure of an Mg-Ca system, showing that $CaMg_2$ Laves phase is ductile with a structural stability. However, there is no report about the experimental values of Debye temperature and the effect of pressure on structural, elastic and electronic properties of $CaMg_2$ Laves phase. In this work, the first-principles calculations are used to investigate the anisotropic elasticity and electronic properties of the $CaMg_2$ Laves phase under pressure. Moreover, the density of state (DOS) under different pressure is analysed to insight into the bonding characteristics of $CaMg_2$, and then reveals the underlying structural stability mechanism of $CaMg_2$ Laves phase. The current work can act as a theoretical prediction and provides mechanical parameters of $CaMg_2$ alloy.

2 Theoretical principle and calculation algorithm

---

[a] Corresponding author : fuj@sustc.edu.cn

2.1 Description of elastic constants algorithm and Young's modulus calculation

A multi-particle electronic structure satisfies the Schrödinger equation. Generally, Hamiltonian contains kinetic energy, Coulomb potential energy between electrons and the external potential, which is described as:

$$H=\sum_{i}-\frac{\hbar^{2}}{2m}\nabla_{i}^{2}+\sum_{i,j}{}'\frac{e_{1}^{2}}{\left|\vec{r}_{i}-\vec{r}_{j}\right|}+\sum_{i}V_{i}\left(\vec{r}\right) \tag{1}$$

Where, $V_i(r)$ is an external potential; r_i and r_j are the nucleus position vectors; while mε and m stand respectively for the mass of nuclei and electrons. $\hbar$ is the reduced Planck constant.

Kohn-Sham equation as an approximation to simplify Schrödinger equation is described as[10]:

$$\begin{cases}\left[-\frac{\hbar}{2m}\nabla^{2}+V_{eff}\left(\vec{r}\right)\right]\varphi_{i}\left(\vec{r}\right)=\varepsilon_{i}\varphi_{i}\left(\vec{r}\right)\\ V_{eff}\left(r\right)=V\left(\vec{r}\right)+V_{ee}\left(\vec{r}\right)+V_{ex}\left(\vec{r}\right)\\ V_{xe}\left(\vec{r}\right)=\frac{\delta E_{xe}[\rho]}{\delta\left(\vec{r}\right)}\\ \rho\left(\vec{r}\right)=\sum_{i}\left|\phi_{i}\left(\vec{r}\right)\right|^{2}\end{cases} \tag{2}$$

Where, $V_{xe}\left(\vec{r}\right)$ is an exchange-correlation potential; $\rho\left(\vec{r}\right)$ is the electron density. Equation (2) includes not only the nucleus and electron kinetic energy term but also term of nucleus- nucleus and electron-electron interactions[10]. The electron density is optimised and elastic constants are obtained.

For hexagonal structure, mechanical stability condition and Voigt/ Reuss bounds of *B* and *G* are[11]:

$$C_{11}>0;C_{11}-C_{12}>0;C_{44}>0;(C_{11}+C_{12})C_{33}-2C_{13}^{2}>0 \tag{3}$$

$$B_{V}=\frac{2}{9}(C_{11}+C_{12}+\frac{1}{2}C_{33}+2C_{13})\,;\;G_{V}=\frac{1}{30}(7C_{11}-5C_{12}+12C_{44}+2C_{33}-4C_{13}) \tag{4}$$

$$B_{R}=\frac{(C_{11}+C_{12})-2C_{13}^{2}}{C_{11}+C_{12}+2C_{33}-4C_{13}}\,;\qquad G_{R}=\frac{5}{2}\left\{\frac{[(C_{11}+C_{12})C_{33}-2C_{13}^{2}]C_{44}C_{66}}{3B_{V}C_{44}C_{66}+[(C_{11}+C_{12})C_{33}-2C_{13}^{2}](C_{44}+C_{66})}\right\} \tag{5}$$

Then homogenized elastic properties of polycrystals can be derived. Shear and bulk moduli are obtained by means of Voigt and Reuss bounds, which are based on the C_{ij} calculated. Then the Voigt-Reuss-Hill average and Young's modulus can be determined from shear/bulk modulus[11].

Based on C_{ij}, Debye temperatures can be estimated by the some sound velocity equations[12]:

$$\Theta_{D}=\frac{h}{k_{B}}\left[\frac{3n}{4\pi}\left(\frac{N_{A}\rho}{M}\right)\right]^{1/3}V_{m}\,,\;V_{m}=\left[\frac{1}{3}\left(\frac{2}{V_{s}^{3}}+\frac{1}{V_{l}^{3}}\right)\right]^{-1/3},\;V_{s}=\sqrt{\frac{G}{\rho}}\,,\;V_{l}=\sqrt{\left(B+\frac{4}{3}G\right)\frac{1}{\rho}} \tag{6}$$

Where Θ_D is Debye temperature; *h* and k_B are the Planck and Boltzmann constant; *n* the total number of atoms; ρ is density; N_A the Avogadro number; *M* the molecular weight per formula; V_m the average sound velocity; V_s the transverse sound velocity and V_l the longitudinal sound velocity.

2.2 Desription of CaMg2 modeling and computational method

Fig.1 shows $CaMg_2$ crystal of hexagonal structure with a space group P63/mmc. Ca atoms are located on *4f* sites and Mg atoms *2a*, *6f* sites. Pseudo atomic calculations are performed for Mg *2p6 3s2* and Ca *3s2 3p6 4s2*.

Crystal lattice ($a=b=6.250$Å, $c=10.101$Å, $\alpha=\beta=90°$, $\gamma=120°$) is shown in Fig.1 a). DFT calculation is shown in Fig.1 b), initial conditions are as: the exchange-correlation function is generalized gradient approximation (GGA); Cutoff energy of the plane waves for ultrasoft pseudopotentials is 400 *eV*.

Brillouin zone is 12×12×8 by Monkhorst-Pack method. The self-consistent convergence of the total energy is $5.0\times10^{-6}eV$ per atom and convergence of the force on all atoms is less than 0.001eV/nm, the pressure region is 0～60*GPa*.

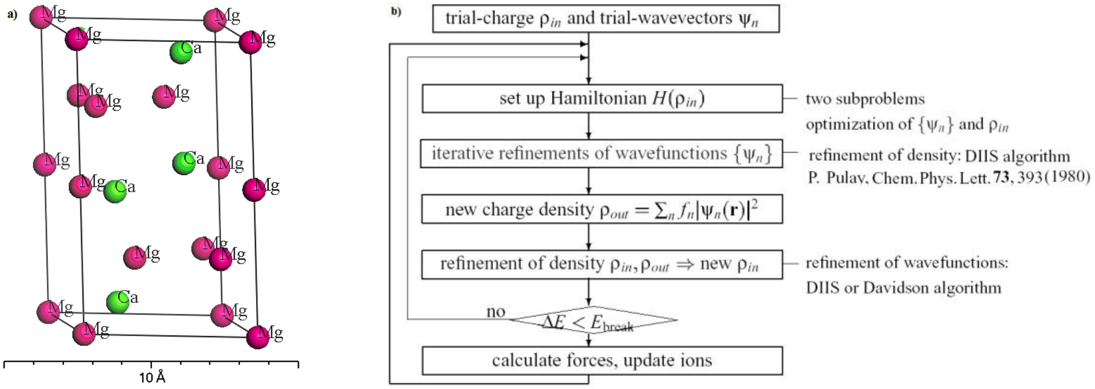

Figure.1 a) Final parameters of $CaMg_2$ crystal; b) Flowchart of DFT by solving Kohn-Sham equations

3 Results and discussion

3.1 Structural parameters and elastic constants

The equilibrium lattice parameters, elastic constants C_{ij} and bulk modulus B_0 are in Tab.1.

Table.1 The structural parameters (a_0, c_0, c_0/a_0, V_0), elastic constants and bulk modulus B_0 of $CaMg_2$ phase at 0GPa.

a) Lattice parameters

	a_0(Å)	c_0(Å)	c_0/a_0	V_0(Å^3)
This work	6.250	10.101	1.616	341.732
Cal.[10]	6.240	10.140	1.625	342.200
Cal.[2]	6.232	10.093	1.620	339.740
Exp.[7]	6.220	10.100	1.624	341.081

b) Elastic constants

	C_{11}	C_{12},	C_{13}	C_{33}	C_{44}
This work	55.70	18.05	15.26	58.39	16.95
Cal.[9]	51.43	22.31	14.73	58.51	14.32
Cal.[3]	62.95	15.27	13.64	65.20	17.77

As the values in Tab.1 match well with experimental values, it is indicated that the present model is reliable. Variations of lattice parameter and elastic constants with increase of pressure are in Fig.2.

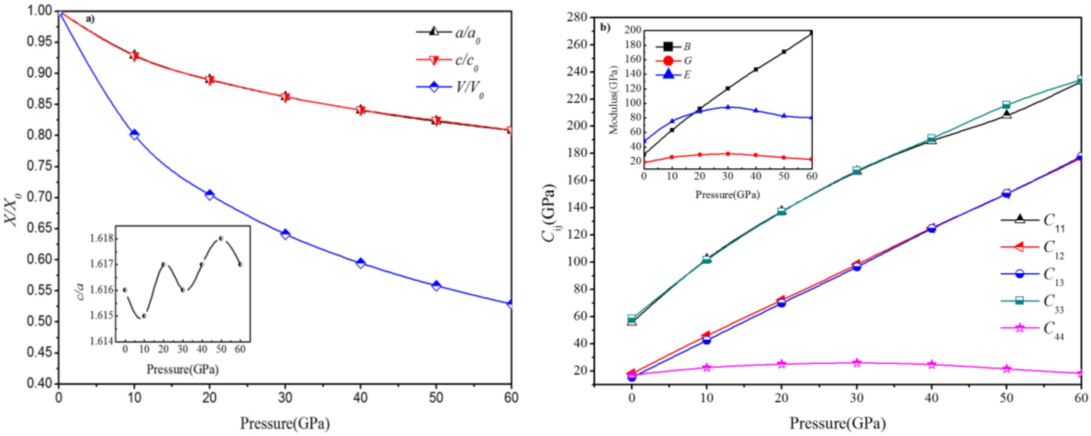

Figure.2 Parametres under pressure of 0- 60GPa: a) Relative change of a, c and V; b) Elastic constants C_{ij}.

As shown in Fig.2 a), it can be seen that $CaMg_2$ has not undergone a phase transition according to the smooth variation of a/a_0, c/c_0 and V/V_0 with the increase of pressure. Moreover, it shows that the lattice parameter a and parameter c are almost equal throughout the whole pressure range, indicating that the elastic anisotropy of $CaMg_2$ is weak. The compressive ability of $CaMg_2$ crystal under pressure is consistent with the variation trend of the V/V_0 curve. The axial ratio c/a changes little with increase of pressure, from minimum 1.615 to maximum 1.618. As in Fig. 2 b), we can conclude that C_{11} and C_{33} are more sensitive to the change of applied pressure than C_{12} and C_{13}. Besides, the applied pressure has less effect on C_{44} and G, while C_{11}, C_{12}, C_{13}, C_{33}, bulk and Young's modulus show the increasing tendency with the increase of pressures.

3.2 Prediction of elastic moduli of CaMg2 ploycrystals

To investigate the effect of the applied pressure on structural properties of $CaMg_2$, The changes of Poisson's ratio and G/B with increasing pressure are plotted in Fig.3

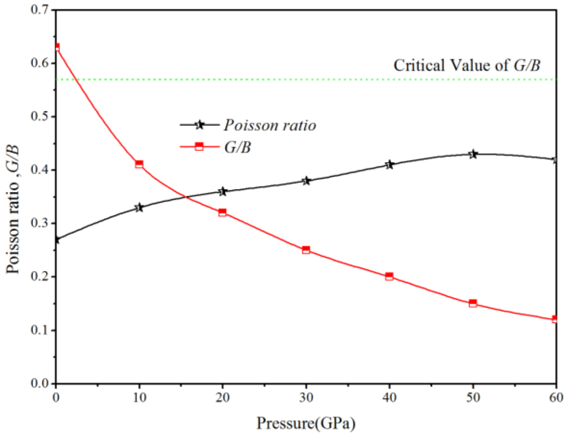

Figure.3 The pressure independence of Poisson's ratio and the G/B ratio of $CaMg_2$

As shown in Fig.3, the G/B ratio decreases with the increasing pressure. Poisson's ratio at 0*GPa* is 0.27, showing CaMg2 is with predominantly central interatomic forces. The critical value which separates brittleness and ductility is about 0.57 in the horizontal dotted line. Evidently, the G/B ratio within region of 0～4*GPa* is higher than critical value 0.57 at 4*GPa*, which implies that $CaMg_2$ phase show a little brittle at 0*GPa* (G/B =0.63) and turn to be a ductile behavior after critical value. It is indicated that $CaMg_2$ shows slight brittleness under 0～4*GPa* and good ductility under 4～60*GPa*.

3.3 Analysis of the density of state (DOS) and bonding characteristics

Fig.4 shows the total and partial DOS of $CaMg_2$ phase near Fermi level under 0*GPa* in Fig.4 a), 20*GPa* in Fig.4 b), 40*GPa* in Fig.4 c) and 60*GPa* in Fig.4 d).

As in Fig.4, the total DOS of $CaMg_2$ is mainly made up of the *s, p* states of Mg atoms below Fermi level and the *s*, *p* states of Ca atoms above Fermi level. It is evident that the total DOS of $CaMg_2$ decreases with elevated pressure, which implies that applied pressure is of benefit to the stability of $CaMg_2$. Moreover, $CaMg_2$ is characterised to have the metallic behaviour as there is no energy gap near the Fermi level[2,6,8,9]. The main bonding peak is located in the energy region from -2 to 4eV, originated from the contribution of valence electron numbers of Mg *s*, Mg *p*, Ca *s* and Ca *p* orbits. A hybridization of Mg *s*, *p* and Ca *s*, *p* orbits is seen in Fig.4 a), indicating the existence of covalent bonding in $CaMg_2$ crystal. From Fig.4 b) to Fig.4 d), the shifting of Mg *s* and *p* orbits from higher to lower energy region is discovered. Moreover, with increasing pressure, the Ca *s* and *p* orbits present a slight broadening and a decrease of intensity, which indicates that the hybridization of Mg *s, p* and Ca *s, p* orbits is becoming stronger. It is worthwhile to note that the applied pressure has a little effect on the DOS when the pressure is above 40*GPa*.

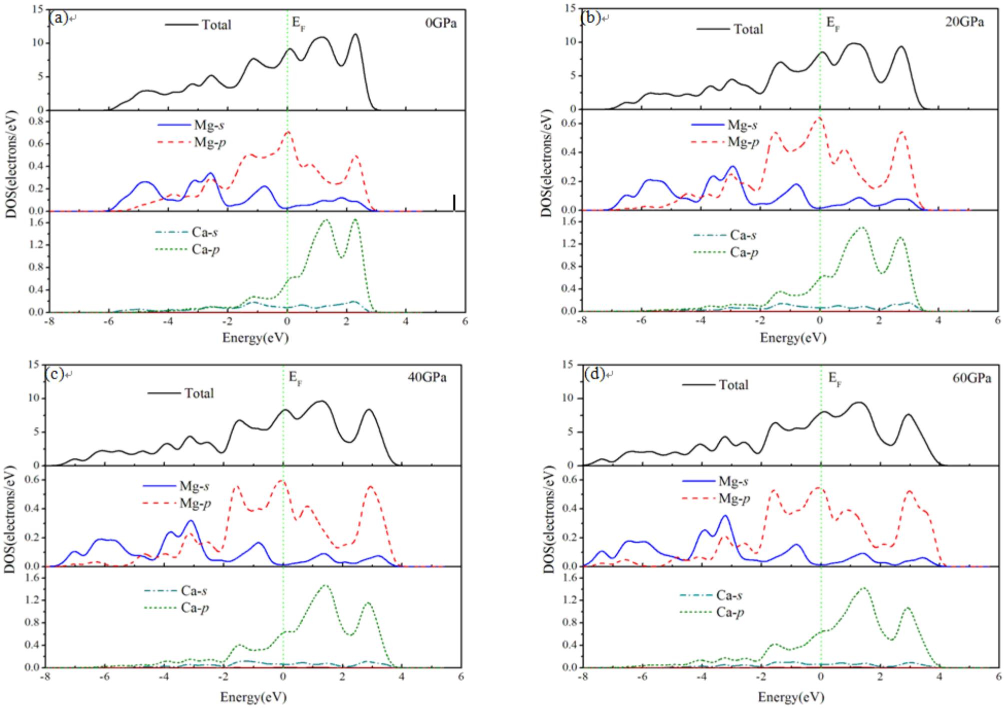

Figure.4 The total and partial density of states (DOS) of CaMg2: a) at 0GPa; b) at 20 GPa; c) at 40 GPa; d) at 60 GPa.

3.4 Analysis of Mulliken electron population and Debye temperature

The Mulliken electron population has been performed to consider the ionic bond feature of $CaMg_2$ phase. Table 4 shows the Mulliken electron population of $CaMg_2$ under pressure.

Table 2: a) Mulliken electron population of pressure; b) Pressure dependence of parameter ρ , V_s, V_l, V_m and Θ_D

Pressure(GPa)	Species	s	p	d	Total	Charge (e)
0	Ca	2.44	6.00	0.66	9.10	0.90
	Mg (I)	0.92	7.45	0.00	8.37	-0.37
	Mg (II)	0.93	7.55	0.00	8.48	-0.48
30	Ca	2.32	5.98	1.00	9.30	0.70
	Mg (I)	0.89	7.31	0.00	8.20	-0.20
	Mg (II)	0.90	7.50	0.00	8.40	-0.40
60	Ca	2.27	5.96	1.25	9.48	0.52
	Mg (I)	0.93	7.09	0.00	8.02	-0.02
	Mg (II)	0.95	7.39	0.00	8.34	-0.34

Pressure (GPa)	ρ (kg/m^3)	V_s (m/s)	V_l (m/s)	V_m (m/s)	Θ_D (K)
0	1.724×10^3	3277.83	5614.24	3635.41	348.70
10	2.150×10^3	3470.14	6249.48	3865.02	399.02
20	2.447×10^3	3462.69	7288.72	3895.40	419.86
30	2.688×10^3	3372.35	7744.53	3808.73	423.56
40	2.898×10^3	3151.89	7987.80	3571.81	407.29
50	3.086×10^3	2886.38	8146.42	3279.92	381.92
60	3.260×10^3	2656.17	8420.52	3024.84	358.71

(Note: ρ is density, V_s transverse sound velocity, V_l longitudinal sound velocity, V_m average sound velocity, Θ_D Debye temperature.)

As in Tab.2 a), the total charge transfer from Ca atoms to Mg atoms at 0*GPa* is 3.60, at 30*GPa* is 2.80 and at 60*GPa* is 2.08. The charge transfer from Ca atoms to Mg atoms demonstrates the ionic bonding in $CaMg_2$ crystal. It is found that the charge transfer from Ca to Mg decreases with the increasing pressure, implying that the ionic bonding is getting weaker[8] under the higher pressure.

Tab.2 b) has listed the calculated V_s, V_l, V_m and Θ_D from 0～60 GPa of $CaMg_2$. Debye temperature at 0 GPa is 348.70 K, and it is clear that the Debye temperature increases under 0～30*GPa* with increasingly applied pressure then presents a declining trend when the applied pressure is above 30*GPa*.

4 Conclusions

Structural, elastic and electronic properties of $CaMg_2$ Laves phase under external pressure from 0～60*GPa* are investigated by DFT. Conclusions are as follows:

1) The optimized structural parameters (a=b=6.250Å, c=10.101Å, V=341.732 Å^3) are very close to experimental values. From DFT calculation, $CaMg_2$ Laves phase under 0～60GPa does not undergo a phase transition, and the compressibility in *a* direction is better than in *c* direction.

2) Based on elastic constants by DFT, the mechanical parameters of $CaMg_2$ are as: bulk modulus is 29.659*GPa*, shear modulus 18.553*GPa*, Young's modulus 49.286*GPa*, Poisson's ratio 0.196 and elastic anisotropy factor *A*. The *G/B* ratio shows a decreasing tendency with the increase of pressure.

3) From DOS analysis at 0, 20, 40 and 60*GPa* show that below Fermi level the total DOS is mainly Mg *s*, *p* orbits while above Fermi level the total DOS is almost Ca *s*, *p* orbits. Moreover, covalent bonding is existed in CaMg2 crystal according to the orbital hybridization of Mg *s*, *p* and Ca *s*, *p* orbits. Mulliken electronic population demonstrate the charge transfer from Ca to Mg becomes less thus the ionic bond between Ca and Mg becomes weaker with the increase of pressure.

4) The Debye temperature shows an increasing tendency with the applied pressure from 0 ～30

GPa and then presents a declining tendency under the pressure region of 30 GPa～60GPa.

References

1. Z.B. Sajuri, T. Umehara,Y. Miyashita et al., Advanced Engineering Materials, **5** (2003) 910-916.
2. B.Y. Tang, W.Y.Yu, X.Q. Zeng et al., Materials Science and Engineering: A, **489** (2008) 444.
3. B.L. Mordike, T. Ebert, Materials Science and Engineering: A, **302** (2001) 37–45.
4. K.Oh-Ishi, C.L.Mendis, T.Homma, S.Kamado et al., Acta Materialia, **57** (2009)5593-5604.
5. J.F. Fan, G.C. Yang et al., Chinese Journal of Nonferrous Metals, 2004, **14** (10):1666-1670.
6. P. Zhou et al., Journal of the Mechanical Behavior of Biomedical Materials, **8** (2012) 154-164.
7. K. Aonol, S. Orimo, H. Fujii, Journal of Alloys and Compounds., **309** (1-2), (2000),L1-L4.
8. A. Suzuki, N.D. Saddock, J.W. Jones, T.M. Pollock, Acta Materialia, **53** (2005) 2823-2834.
9. W.Y. Yu, N.Wang, X.B. Xiao, B.Y. Tang et al., Solid State Sciences, **11** (2009):1400.
10. Aaeid A., PhD Thesis, l’Université des Sciences et Technologies de Lille, 2010 France. (French)
11. Wu Z J et al., Physical Review B, **76** (2007), 054115
12. O.L.Anderson, Journal of Physics and Chemistry of Solids, **24** (1963) 909.